Bulletin of the Geological Survey of Japan, vol. 43 (1/2), p. 31-41, 1992

Interpretation of the Matsumoto Basin gravity low

Tom WILSON* and Hirokazu KATO**

WILSON, Tom and KATO, Hirokazu (1992) Interpretation of the Matsumoto Basin gravity low. *Bull. Geol. Surv. Japan,* vol. 43 (1/2), p. 31-41, 8 fig.

Abstract: It has been suggested that the gravity low over the Matsumoto Basin is associated with a reverse fault where the northeast side has been thrust upwards by nearly 4 km or more. Gravity models presented in this study suggest that the low in the Bouguer gravity observed across this basin is produced by a graben-like low density distribution and that the boundaries or flanks of this low density area both dip to the southwest, rather than to the northeast. Inverse models derived from residual Bouguer gravity data also suggest that this low density region extends from the near-surface to depths of 4 kilometers or more. The models although non-unique are consistent with nearby seismic refraction data, which also reveal the presence of a laterally restricted low velocity (and therefore low density) region beneath the basin.

This graben-like low density region is interpreted to reflect the presence of a restricted basin and possible deeper fault zone, which is bordered by the Itoigawa-Shizuoka Tectonic Line to the southwest, and the Matsumoto Bonchi Toen Fault to the northeast. The interpreted southwesterly dip of this low density region suggests a reverse sense of motion for the relative uplift of the Hida Mountains by more than 1 kilometer with respect to the bordering Fossa Magna region.

Introduction

The Matsumoto Basin is situated at the western marginal area of the Fossa Magna (Figure 1). The Fossa Magna is a mega-scale half-graben-like depression that developed during Neogene time in the area separating northeastern and southwestern Japan. The basin itself is divided internally into several smaller graben-like structures. The western margin is composed of several north-south trending faults. The extent of these faults are in many cases obscured by fan deposits resulting from relative uplift of the northern Japan Alps (Hida Mountains) by more than 1 kilometer during the Quaternary. The eastern margin of the basin is an active fault named the "Matsumoto Bonchi Toen Fault" (hereinafter referred to as the "MBTF") (Hirabayashi, 1971). This fault plane is nearly vertical and the eastern side of the fault is up. The Itoigawa-Shizuoka Tectonic Line (hereinafter referred to as the "ISTL") is a large-scale fault crossing the main part of Japan. It is regarded as the western boundary of the Fossa Magna in a broad sense. The ISTL passes through the central portion of the Matsumoto Basin along its length, is covered by thick alluvial fan deposits, and is not observed at the surface in this area. Based on a refraction seismic profile across the basin (Yamada, 1969), the ISTL does not appear to affect Pleistocene and younger formations. This implies that the ISTL has been inactive since the early Pleistocene, and during the development of the Matsumoto Basin.

* STA Fellow, West Virginia University, Morgantown, West Virginia, U. S. A.
** Geology Department

Keywords: Matsumoto Basin, Itoigawa-Shizuoka Tectonic Line, Fossa Magna, gravity

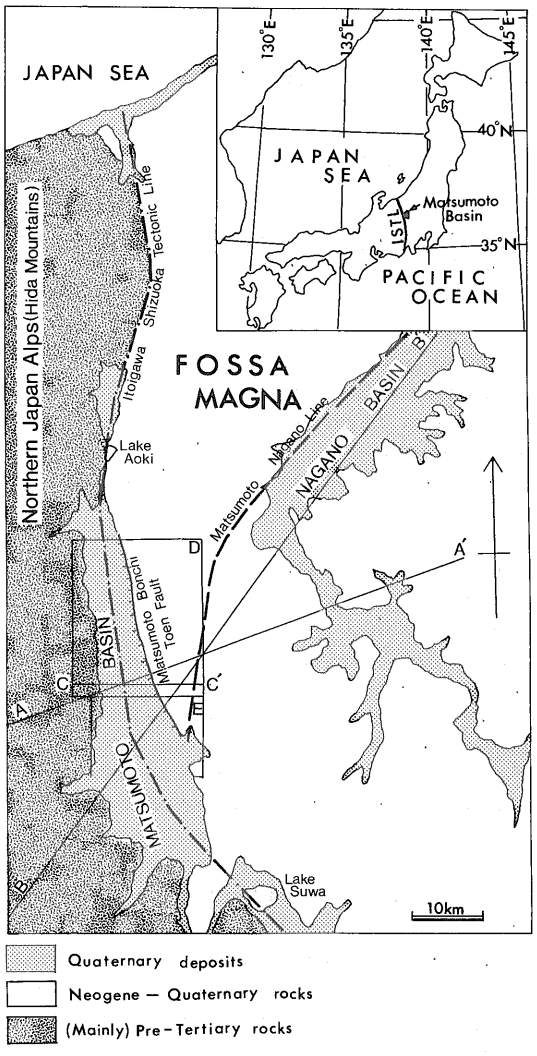

Figure 1 Index map showing study area around the Matsumoto Basin. A–A′ : Wilson and Kato (1991, this study), B–B′ : Ikami *et al.* (1986), C–C′ : Yamada (1968), D : Okubo *et al.* (1990), E : Hagiwara *et al.* (1986).

It has been argued (Hagiwara *et al.*, 1986 ; Okubo *et al.*, 1990) that the steep drop off of the Bouguer anomaly over the Matsumoto Basin implies that the sense of motion along the Matsumoto Bonchi Toen Fault is reversed. Their interpretation therefore suggests that this low density region dips to the northeast several kilometers beneath the surface. On the other hand, many authors (for example, Nakamura, 1983 ; Kobayashi, 1983) have suggested that the ISTL is a plate boundary along which northeastern Japan is subducting beneath southwestern Japan. In this case, one would expect the low density region to dip to the southwest beneath southwestern Japan. The purpose of this paper is to test these hypothesis by presenting gravity models to illustrate the effects on the gravitational field produced by different configurations of subsurface density contrast beneath the area.

A refraction seismic profile across the Matsumoto Basin presented by Ikami *et al.* (1986) reveals the presence of a low velocity region beneath the Matsumoto Basin (Figures 1 and 2). Velocity/density relationships (Ludwig *et al.* 1970) suggest that the density contrast associated with this low velocity region is approximately −0.35 g/cc. We derived simplified density models for a profile across the basin (Figures 1, 3 and 4) using data from Kono and Furuse (1989) and Komazawa *et al.* (in prep.). These inverse models were derived from the residual Bouguer anomaly using an iterative procedure (Inman, 1985) to minimize the difference between the calculated and observed gravity. Only the very long wavelength features (wavelengths greater than 150 km) were removed to obtain these residuals.

The models derived from both gravity data sets (Figures 3 and 4) suggest that the anomaly is produced by a graben-like low density feature, and that the southwest and northeast walls of this graben dip to the southwest. This southwest dip is opposite to that suggested by Ikami *et al.* (1986) based on their seismic refraction data. However, the margins of this low density region are noted as uncertain in their interpretation. The interpretation of refractor dip in this area is complicated because the refraction profile crosses the basin at a high angle.

We note also that the modeled gravity profile and the seismic refraction line do not coincide (Figure 1). The orientation of the gravity profile coincides with that discussed by Okubo *et al.* (1990) and is oriented normal to the trend of the Bouguer anomaly in that area.

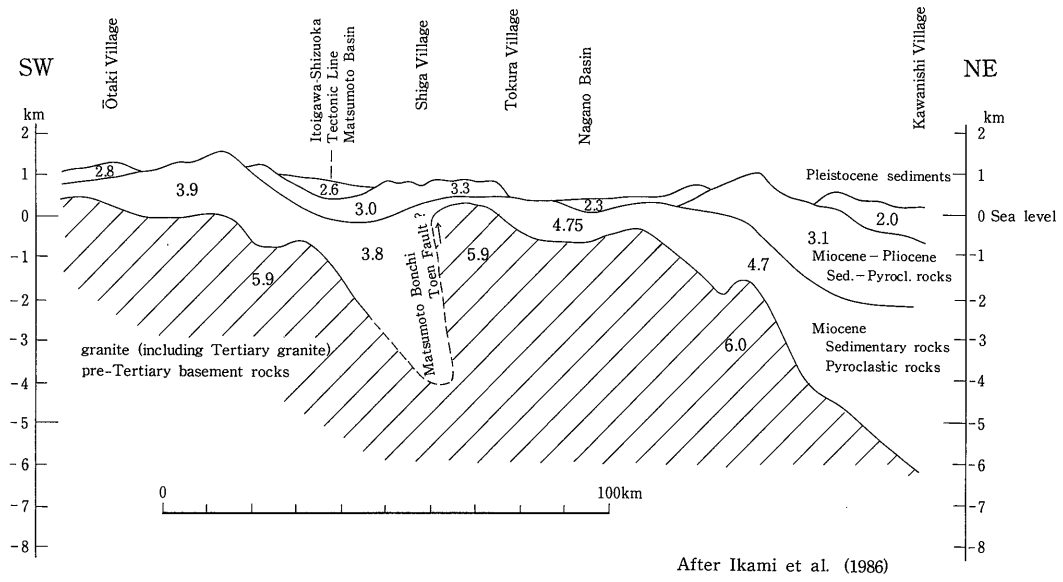

Figure 2 The velocity model presented in this figure is from Ikami *et al.* (1986). The geological interpretation of these intervals is taken from Kato (in prep.).

The gravity and refraction profiles cross about 10 kilometers to the east of the Matsumoto Basin. Greatest similarity between the gravity models and the seismic refraction model occurs in the vicinity of the Matsumoto Basin where the two data sets nearly coincide. Disagreement between the refraction model and the gravity models away from the Matsumoto area to the southwest is expected as the two data sets diverge from each other.

The outcrop pattern of the latest Pleistocene Matsumoto Bonchi Toen Fault (Kato and Sato, 1983) indicates that, in the near-surface, this fault is almost vertical. However, the inference that the deeper (Pliocene to early-Middle Pleistocene) extension of this fault was also reversed, or northeast dipping, is not consistent with the historical development of the area as inferred from surface mapping. Hence, since the main arguments favoring fault reversal along the Matsumoto Bonchi Toen Fault are based on the gravity data (Hagiwara *et al.*, 1986 ; Okubo *et al.*, 1990), we present additional arguments suggesting that such inferences are in fact incorrect for the Matsumoto Basin area.

Gravity Model Studies

Hagiwara *et al.* (1986) suggest that the steepness of the gravity anomaly across the Matsumoto Bonchi Toen Fault implies that offset along this fault is reverse. Their argument is based on a fault step model (Figure 5). They note that fault reversal produces the steepest gravity gradient. However, the refraction derived model presented by Ikami *et al.* (1986) and the gravity models presented in Figures 3 and 4 are consistent in suggesting that the low velocity or low density feature is limited to the region beneath the Matsumoto Basin, and extends to depths of 3 or more kilometers beneath the surface. Relatively high velocity or high density intervals bound this low density region to the southwest and northeast, so that this feature has the structural characteristics of a graben, rather than an isolated fault step.

Hence, we use model studies to evaluate whether the dip of the graben walls, or other characteristics of the graben's configuration will have a greater influence on steepening of

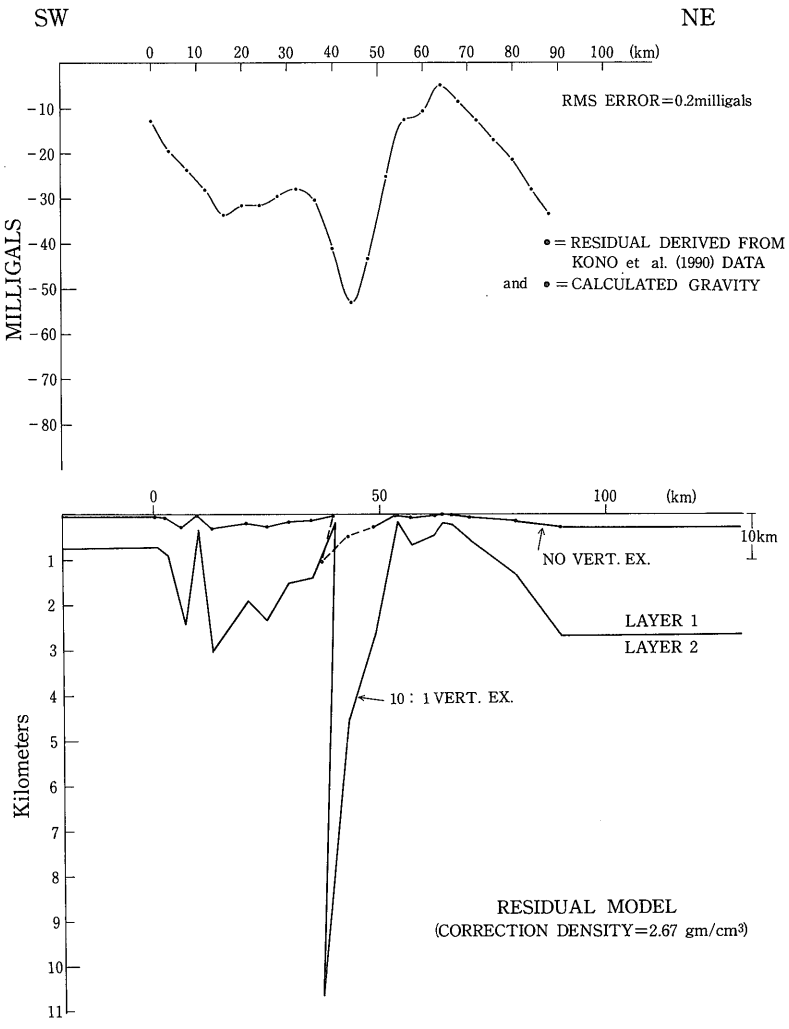

Figure 3 The model shown here (bottom) was derived from the residual Bouguer gravity data at the top. The residual was derived from the data presented in Kono *et al.* (1990) using a filter separation technique. Wavelengths greater than 150 kilometers have been retained. The RMS error between the residual and calculated gravity is 0.2 milligals. The model plotted at a scale of 10 : 1 and 1 : 1.

the gravity anomaly associated with it. Specifically, we examine the effect of variable graben depth, graben width, and the dip of the graben flanks.

Graben Depth

The effects of variations in graben depth on anomaly shape is illustrated in Figure 6. In these models, depth to the floor of the graben beneath the surface is increased from 2.5 to 5.5 kilometers in one kilometer increments. The top of the graben is 0.5 kilometers beneath the surface. Maximum horizontal gradients (dg/dx) and maximum relative anomaly (maximum minus the minimum or base line value) are tabulated in the figure.

Steepest horizontal gradients occur directly over the margins of the graben located at 28 or

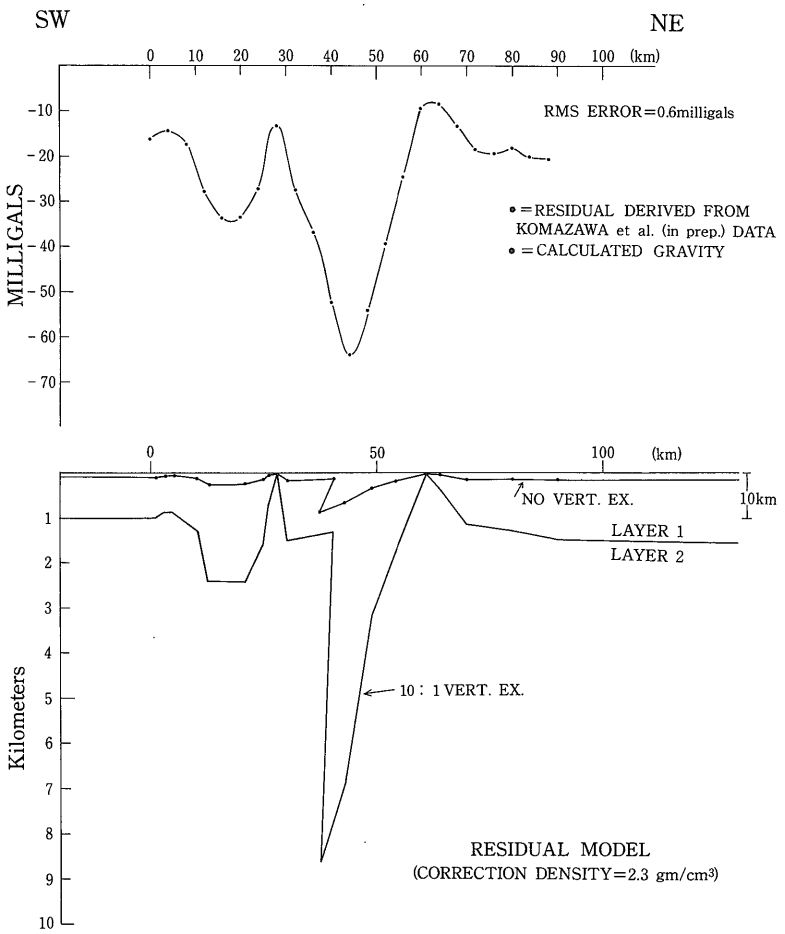

Figure 4 This density model (bottom) was derived from the residual Bouguer gravity data shown at the top. The residual was derived from the data presented in Komazawa *et al.* (in prep.) using a filter separation technique. Wavelengths greater than 150 kilometers have been retained. The RMS error between the residual and calculated gravity is 0.6 milligals. The model plotted at a scale of 10 : 1 and 1 : 1.

42 kilometers along the surface. Doubling the depth of the graben (2.5 to 4.5 kilometers beneath the surface) produces an 80% increase in the amplitude of the anomaly and a 52% increase in the horizontal gradient over the edges of the graben.

Graben Width

The effects of varying the width of the graben are illustrated in Figure 7. The width of the graben is varied from 6 kilometers to 18 kilometers in 4 kilometer increments. Graben depth is held constant at 3.5 kilometers (4 km subsurface). Maximum horizontal gradient over the edges of the graben and maximum relative amplitude are tabulated in the figure for each case.

A 12% increase in the vertical gradient occurs with an increase in graben width from 6 to 10 kilometers, while the amplitude of the anomaly increases by 21%. Successive increases in graben width by 4 kilometer increments produce increases in the horizontal gradient of 1% or less. Successive increases in the gradient appear constant because of round-off. As expected, the half-width of the anomaly corresponds closely to the width of the graben, and becomes nearly exact as the graben width

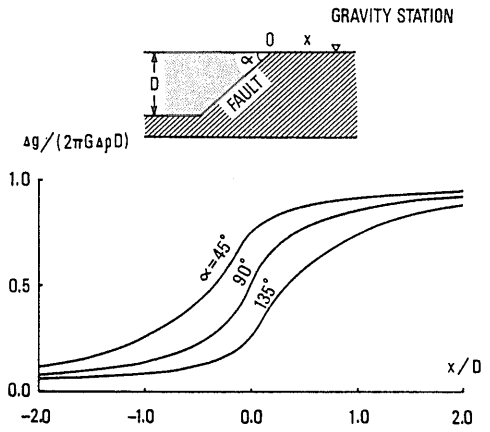

Figure 5 This figure from Hagiwara *et al.* (1986) illustrates the gravity anomaly associated with an isolated fault. Results are shown for normal, vertical and reverse fault orientations.

increases.

Moving the left side of the graben out to minus infinity, yields a simple vertical fault model (down to the left). Calculations for this model are also shown for reference in Figure 7. The vertical gradient for this case is only 1.8% higher than that for the graben with an 18 kilometer width.

Varying the Inclination of a Graben Wall

The effect on the horizontal gradient produced by normal, reverse of vertical offsets across an isolated fault are clearly demonstrated in Figure 5 (from Hagiwara *et al.*, 1986). Whether a similar effect is produced for varying inclinations of one wall of a graben is illustrated in Figure 8.

In Figure 8 we take a graben with 14 kilometer width and 4.5 kilometer depth (5 kilometers subsurface) and vary the inclination

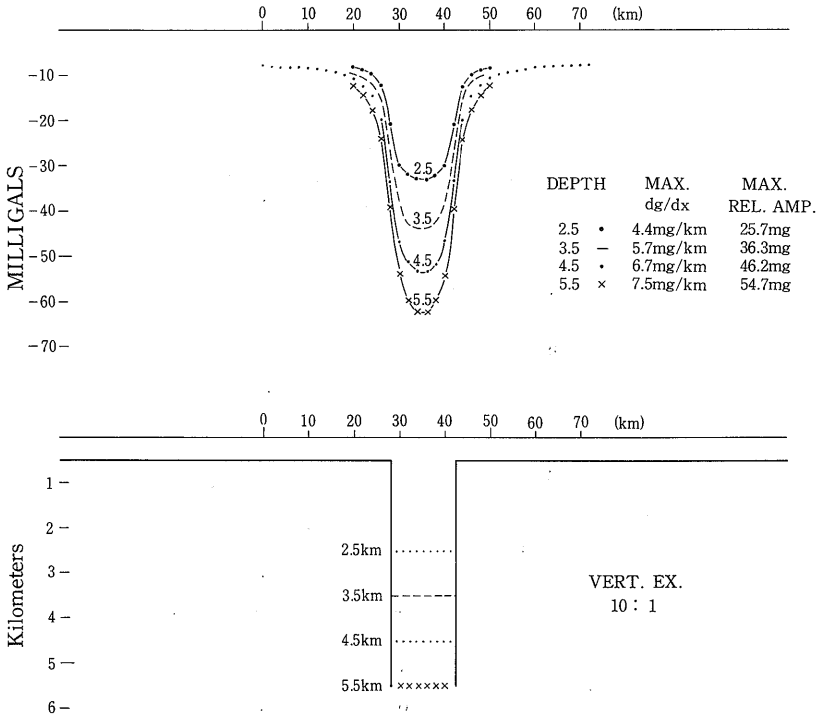

Figure 6 Gravity anomalies are calculated for a simple graben model. Calculations are made to examine the effect of varying the depth to the floor of the graben. A strike-length of 50 km was used in the calculations. The model is presented at a 10 : 1 scale.

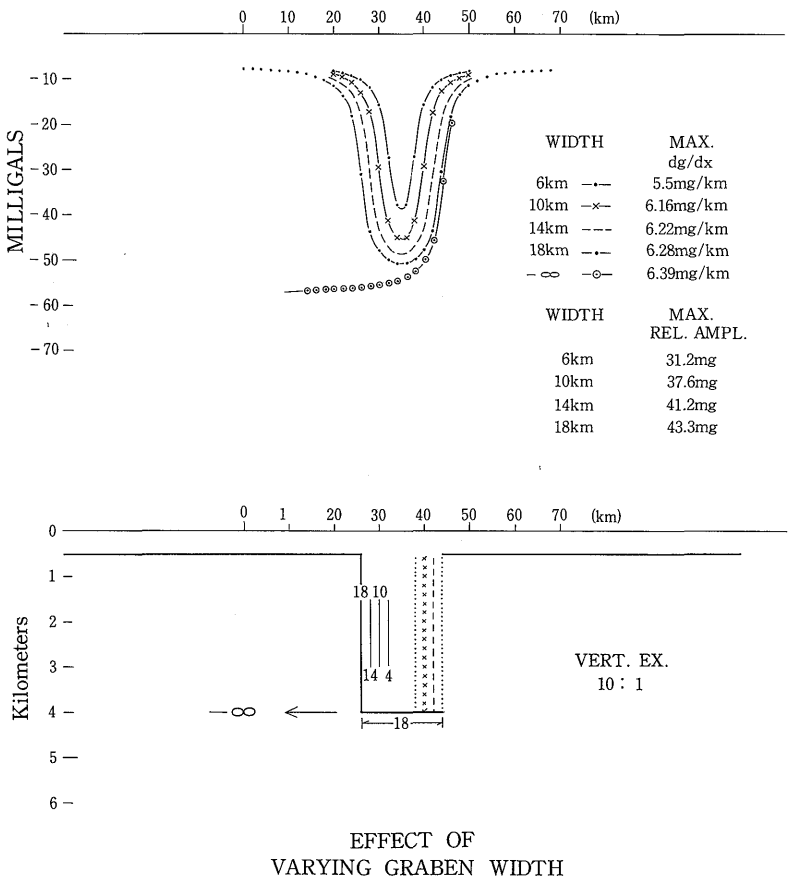

Figure 7 The effect of varying the width of a simple graben is presented for several different graben widths. The isolated fault case is also shown as a limiting case of infinite graben width. The model is presented at a scale of 10 : 1. The strike-length of the graben is 50 kilometers.

of the right wall of the graben from steeply left-dipping through vertical, to steeply right-dipping orientations. The calculations for each case are plotted in the figure, and the maximum vertical gradient of the calculated anomaly over the right flank is tabulated for each case.

The 72 degree maximum dip is simply the dip obtained when the base of the right side of the graben meets the base of the left side for a graben of this width and depth. The intermediate value of 52 degrees is chosen to approximate the dip shown on the subsurface interpretation of refraction data presented by Ikami *et al.* (1986) (figure 2).

The results reveal that the horizontal gradient is greatest when the sides of the graben have a vertical orientation. In this particular example vertical orientation of the graben walls produce a horizontal gradient of 7.13 mgals/km. Inclination to the right or left decreases the horizontal gradient by approximately the same amount. Hence, the horizontal gradient for the left-dipping graben wall inclined at 72 degrees is 3.78 mgals/km and that for the right-dipping inclination of 72 degrees, is almost the same or 3.88 mgals/km. The x-location of the point of steepest gradient also shifts from left to right with left-to-right dipping inclinations of the graben wall. This

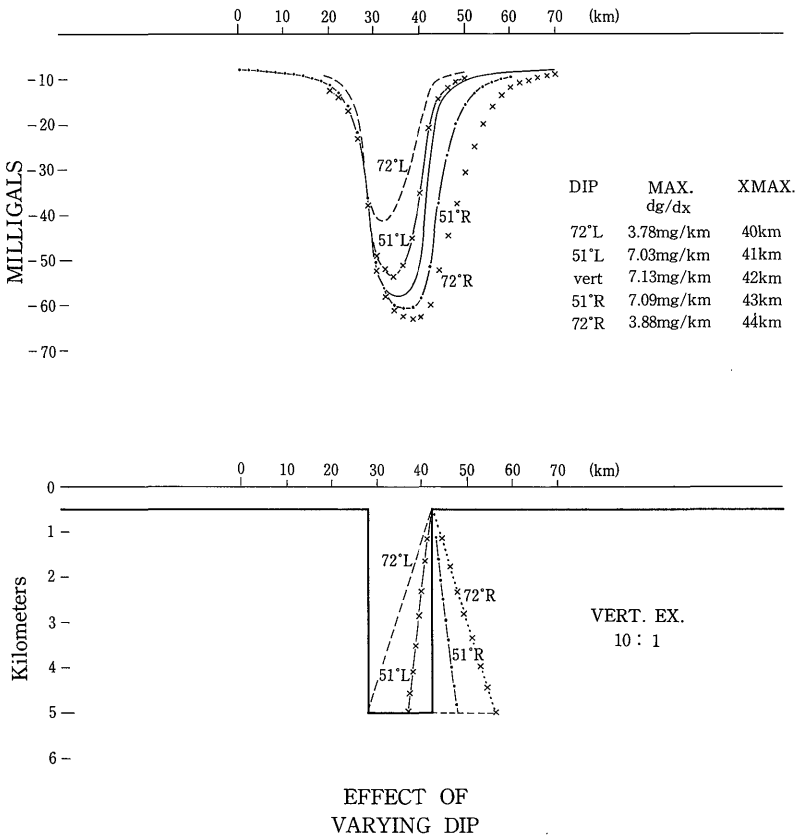

Figure 8 The sense of offset along one flank of the model graben is calculated for normal, reverse, and vertical orientations of the right wall of the graben. The left wall remains vertical. The graben strike-length is 50 kilometers.

point does not lie above the upper right edge of the graben except for the case of vertical orientation.

In addition, the anomaly over the right edge of the graben rises up to baseline values much more gradually as the orientation changes from left to right dipping. To illustrate this we look at the horizontal separation between the location of the anomaly peak and a point where the anomaly reaches −10 milligals beyond the right edge of the graben. This distance increases from 12.5 km for the 72 degrees left-dipping case, to 27 km for the 72 degrees right-dipping case.

Discussion

In the forgoing analysis we have used simplified two-layer models. These models (Figures 3 and 4) are roughly consistent with the deeper velocity structure beneath the area suggested by Ikami *et al.* (1986). Such a simplification might be made under the assumption that the replacement density has successfully removed above-sea level contributions to the anomaly. The variability between the inverse models (Figures 3 and 4) illustrates the limitation of this assumption, since the differences between these two models arise entirely as the result of differences in the replacement density (see Wilson *et al.*, in prep.). Both inverse models consistently suggest that this low density region dips to the southeast.

The forward models (Figures 6–8) presented for a simple graben reveal that varying the inclination of a graben wall from the vertical

in either direction will decrease rather than increase the horizontal gravity gradient across the graben edge. The largest increases in horizontal gradient are produced by increases in the graben depth. For the specific model discussed above (Figure 6), doubling graben depth produces a 52% increase in the horizontal gradient, whereas doubling graben width (Figure 7) produces only a 12.5% increase.

The results also indicate that variations of dip within 50 degrees of vertical (Figure 8), in fact, produce very little change in the horizontal gravity gradient. For instance, orientation of the flank into a right dip of 51 degrees produces only a 1/2 percent change in the horizontal gradient from that associated with the vertical orientation. The main effect of changing flank dip is to shift the point of steepest gradient in the dip direction. The most distinguishing characteristic associated with variable dip of the graben wall is that the roll-off on the high side of the graben edge occurs more gradually as the graben wall is shifted from left-dipping to right-dipping orientations. The roll over is most gradual for the steep right dipping, or "reverse fault" case. This is expected because in the limit that the inclination of the wall becomes horizontal, the wall effectively disappears, and the model becomes equivalent to an isolated vertical fault step such as that shown in Figure 5.

Based on the forgoing analysis (Figures 5–7), the configuration of the low density region inferred by inverse modeling (Figures 3 and 4) is not surprising. The southwest inclination of its northeastern margin may arise because of the relatively short distance over which the anomaly rolls over into the low, rather than to the steepness of the anomaly. The southwest inclination of the southwest boundary of the low density region increases the volume of low density intervals to the southwest and therefore decreases the rate at which the anomaly returns to higher values in the interval 10 to 20 km to the southwest.

We interpret the southwestern edge of the graben-like density feature shown in Figures 3 and 4 as coinciding approximately with the Itoigawa-Shizuoka Tectonic line. Surface geologic mapping of the area reveals that the Hida Mountains southwest of the ISTL have been uplifted by approximately 1 km with respect to formations in the Fossa Magna region northeast of ISTL. Hence, the southwest dip of this low-density zone, as derived from the gravity models, is consistent with the relative reverse sense of motion inferred from geologic mapping (Kato, in prep.). The Himekawa Fault, one of the parallel subsidiary faults of the ISTL to the north of Lake Aoki, is also a reverse fault. That is, the western side of this fault was thrust over the eastern side in Pliocene time. The Himekawa Fault is believed to be the equivalent of the ISTL in this area (Saito, 1978).

The border region separating the Fossa Magna and the Hida Mountains in this area is complex and consists of several faults some of which are currently active. We suggest that the low density region inferred from the gravity models (Figures 3 and 4) and from refraction data of Ikami *et al.* (1986) is a deep basin, which developed within a wide zone of intermittently active faults, some of which are mapped at the surface in the Matsumoto Basin and surrounding areas. Gravity and seismic refraction data are consistent in suggesting that this zone extends to depths of 3 or more kilometers beneath the surface.

The southwest dip of the low density region inferred from the gravity models suggests a reverse sense of offset for the bordering Hida Mountains area with respect to the Fossa Magna. This interpretation does not preclude the presence of local northeast dipping reverse faults within the basin, such as those currently observed along the Matsumoto Bonchi Toen Fault. Although the inverse models presented here are non-unique, they are constrained by seismic refraction data. The interpretations of these models, appear most consistent with the geologic history of the area as inferred from surface mapping and seismic refraction data. This interpretation is also in harmony with the hypothesis that northeastern Japan has undergone partial subduction beneath southwestern Japan, although the ISTL, itself, may

not be the precise boundary between northeastern Japan and southwestern Japan during the Quaternary (Kato, in prep.).

Acknowledgements : Discussions with Dr. Hitoshi HATTORI and Dr. Takanobu YOKOKURA of the Geological Survey of Japan were very helpful. Dr. M. KOMAZAWA allowed us to use unpublished gravity data from the Matsumoto area. This study was sponsored in part through the Japan International Science and Technology Exchange Center. Critical reviews and suggestions by Dr.T. YOKOKURA and Dr.K. KANO were helpful and greatly appreciated.

References

Hagiwara, Y., Yamashita, N., Kosaka, T, Yano, K. and Yasui, T. (1986) Gravity observations along the Itoigawa-Shizuoka Geotectonic line (I)—An evaluation of the Bouguer anomaly in the Matsumoto Basin, Nagano Prefecture, Central Japan. *Bull. Earthq. Res. Inst., Univ. Tokyo*, vol. 61, p. 537–550.

Hirabayashi, T. (1971) Kita azumishi, Chapter 6, Median Lowlands. p. 222–234.

Ikami, A., Yoshii, T., Kubota, S., Sasaki, Y., Hasemi, A., Moriya, T., Miyamachi, H., Matsu'ura, R. and Wada, K. (1986) A seismic refraction profile in and around Nagano Prefecture, central Japan. *Jour. Phys. Earth,* vol. 34, p. 457–474.

Inman, J.R. (1985) Resistivity inversion with ridge regression. *Classic Paper*, vol. 50, p. 2112–2131.

Kato, H. (1992) Fossa Magna—A masked border region separating southwest and northeast Japan. *Bull. Geol. Surv. Japan.* vol. 43, p. 1–30.

——— and Sato, T. (1983) *Geology of the Shinano-Ikeda District.* Quadrangle Series, Scale 1 : 50,000, Geol. Surv. of Japan, 93 p.

Kobayashi, Y. (1983) On the initiation of subduction of plates. *Earth Monthly,* vol. 5, p. 510–514.

Komazawa, M. *et al.* (in prep.) Bouguer gravity map of Japan. 1 : 1 Million scale map.

Kono, Y. and Furuse, N., editors (1989) 1 : 1 Million scale gravity anomaly map in and around the Japanese Islands. Maps and explanatory text. 76 p.

Ludwig, W.J., Nafe, J.E. and Drake, C.L. (1970) Seismic refraction. *In* A.E. Maxwell, ed. *The sea*, vol. 4, Part 1. Wiley-Interscience, New York, p. 53–84.

Nakamura, K. (1983) Possible nascent trench along the Japan Sea as the convergent boundary between Eurasian and North American plates. *Bull. Earthq. Res. Inst.* vol. 58, p. 711–722.

Okubo, S., Nagawasa, K., Murata, I. and Sheu, H. (1990) Gravity observations along the Itoigawa-Shizuoka Geotectonic Line (III)—Bouguer anomaly around the northern part of the Matsumoto Bonchi Toen Fault. *Bull. Earthq. Res. Inst. Univ. Tokyo,* vol. 65, p. 649–663.

Saito, Y. (1978) The Himekawa Fault and the Kozuchiyama Landslide. *Bull. Fac. Educ., Shinshu Univ.*, no. 39, p. 203–214.

Yamada, T. (1968) Itoigawa-Shizuoka Tectonic Line surveyed by seismic prospecting to the north of Matsumoto City. *Fossa Magna,* p. 41–44. Geol. Soc. Japan.

松本盆地低重力の解釈

トム　ウィルソン・加藤碵一

要　　旨

松本盆地の低重力異常は盆地北東側の新第三系からなる中山山地の 4 km ないしそれ以上の上昇による逆断層に関連づけて解釈されてきた．本研究で呈示された重力モデルは，松本盆地で観測された低ブーゲー重力異常が地溝状の低密度分布によって説明可能であることと，この低密度領域の境界がむしろ南西に傾斜していることを示唆している．残留重力データからのインバースモデルもまたこの低密度領域が地表部から 4 km ないしそれ以上の深さまで続くことを示唆している．モデルは，唯一の解ではないけれども，本盆地地下で側方に限定された低速度領域（すなわち低密度領域）の存在を示す近傍の屈折法地震探査データと一致する．この地溝状低密度領域は南西縁を糸魚川-静岡構造線（ないし近傍の並走断層），北東縁を松本盆地東縁断層に境された盆地ないし，より深部の断層帯を反映していると解釈される．また，この低密度領域の南西方への傾斜は飛騨山地側がフォッサ・マグナ地域に対して相対的に 1 km 以上逆断層センスで隆起していることを示唆するが，このことは地質学的な糸魚川-静岡構造線の第四紀における活動を直接意味するものとは限らない．

（受付：1991 年 6 月 24 日；受理：1991 年 7 月 24 日）